JACS
JOURNAL OF THE AMERICAN CHEMICAL SOCIETY

ARTICLE

pubs.acs.org/JACS

Dictyostatin Flexibility Bridges Conformations in Solution and in the β-Tubulin Taxane Binding Site

Ashutosh S. Jogalekar,[†] Krishnan Damodaran,[‡] Frederik H. Kriel,[†] Won-Hyuk Jung,[‡] Ana A. Alcaraz,[†] Shi Zhong,[†] Dennis P. Curran,*[,‡] and James P. Snyder*[,†]

[†]Department of Chemistry, Emory University, 1515 Dickey Drive, Atlanta, Georgia 30322, United States

[‡]Department of Chemistry, University of Pittsburgh, 1101 Chevron Science Center, 219 Parkman Avenue, Pittsburgh, Pennsylvania 15260-3900, United States

Supporting Information

ABSTRACT: Dictyostatin (DCT, **1**) is a complex, flexible polyketide macrolide that demonstrates potent microtubule-polymerization activity. Both a solution structure (**2a**) and a possible binding mode for DCT (Conf-1) have been proposed by earlier NMR experiments. In the present study, the conformational landscape of DCT in DMSO-d_6 and methanol-d_4 was explored using extensive force-field-based conformational searches combined with geometric parameters derived from solution NMR data. The results portray a diversity of conformations for dictyostatin that illustrates the molecule's flexibility and excludes the previously suggested dominant solution conformation **2a**. One conformation present in DMSO-d_6 with a 7% population (Conf-2, 0.6 kcal/mol above the global minimum at 298°) also satisfies the TR-NOESY NMR parameters of Canales et al. that characterize the taxane binding-site interaction between DCT and assembled microtubules in water. Application of several docking methods (Glide, Autodock, and RosettaLigand) has identified a low-energy binding model of the DCT/β-tubulin complex (Pose-2/Conf-2) that is gratifyingly compatible with the emerging DCT structure−activity data.

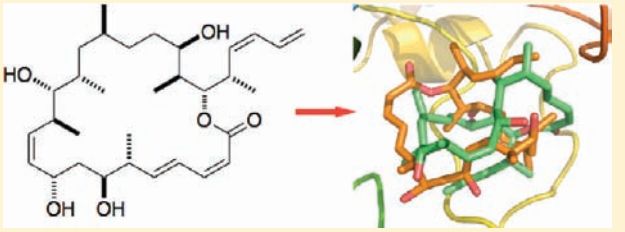

INTRODUCTION

Dictyostatin (**1**, Figure 1, DCT) is a marine macrolide discovered in the Republic of Maldives that inhibits microtubule disassembly. In addition to being a potent competitor at the paclitaxel (PTX) binding site with an action similar to that of discodermolide and other microtubule stabilizing agents, the compound is also effective against PTX-resistant cancer cell lines. Consequently, the compound is regarded as a template for a new class of anticancer agents.[1] Because discodermolide was recently withdrawn from clinical trials as a result of potential lung and liver toxicities,[2] dictyostatin is regarded as a potential anticancer alternative that may evidence fewer damaging side effects. Interest in DCT remains high, with numerous total syntheses of the parent compound and hybrid analogues published recently.[3]

To determine the complete relative stereochemistry of **1**, a Cambridge−Harbor Oceanographic Institution (HOI) team combined high field 2D NMR and Murata's J-based configuration analysis.[4] In addition to stereogenic center assignments, a pair of interconverting conformations, regarded as being relatively rigid in over 60% of the 22-membered ring structure, was proposed by analysis of three-bond proton−proton couplings ($^3J_{H-H}$) and NOESY correlations. A structure for the form presumed to be most populated (**2a**, Figure 2) was obtained by a conformational search with the MM2*/GBSA/H_2O force field.[5] Subsequently, **2a** has been implicated as the possible bioactive entity by overlaying it with the X-ray,[3c,6] preferred

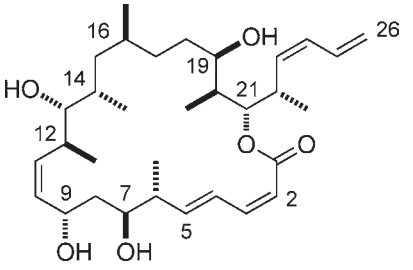

Figure 1. Dictyostatin (**1**, DCT).

solution[7] or proposed bioactive hairpin conformation of discodermolide.[7,8] Structural analysis of the latter has provided insights into the unusual constancy of 3-D shape across all three of these environments,[9] a conformation recently employed in the hydrogen−deuterium exchange (HDX) studies of Horwitz, Smith, and colleagues.[10]

The Cambridge−HOI study on **2a** draws attention for two reasons. First, it seems unlikely that a 22-membered ring in solution will exist as a relatively rigid body with only 20−25% of the structure (C17−C21−C2) interconverting between two dominant rotamers as proposed. While the previous workers acknowledge that the ambient NMR spectrum of **1** is a dynamic

Received: March 22, 2010
Published: February 7, 2011

   dx.doi.org/10.1021/ja1023817 | J. Am. Chem. Soc. 2011, 133, 2427–2436

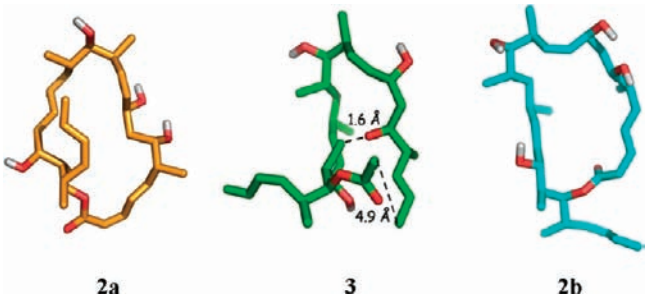

Figure 2. Comparison of the MM2* global minimum **2a** (gold) said to be consistent with the measured $^3J_{H-H}$ values for DCT and **3** (green), a structure derived from the dihedral angles corresponding to the same $^3J_{H-H}$ values (cf., Table S1). For **3**, this leads to a 4.9 Å gap separating two otherwise bound carbons (C2−C3). Structure **3** also sustains a 1.6 Å cross-molecule steric clash between the C7−O hydroxy oxygen and the C20−C methyl carbon. Comparison of unsaturated lactone *s-trans* unsaturated lactone **2a** and *s-cis* unsaturated lactone **2b** illustrates the lactone carbonyls to reside outside and inside the average macrocyclic rings, respectively.

average, it appears that two conformational candidates have been extracted from a much more complex set of conformers. Second, even a tentative acceptance of the assumption that such a conformation might be the bioactive one could prove misleading as it did in the pursuit of constrained analogues of paclitaxel. In that case, a body of synthetic chemistry was devoted to preparing analogues of presumed bioactive conformers, few of which proved to match PTX potency.[11]

Recently, β-tubulin-bound structures of both discodermolide (DDM)[8,12] and dictyostatin[12] ligands have been determined by transferred NOE NMR spectroscopy. Structures for DDM have also been proposed by HDX[10] and modeling[9] methods. Unlike discodermolide but like most other protein-bound ligands, dictyostatin in solution and in complex with tubulin presents two quite different conformations.[12] To investigate the conformational behavior of dictyostatin more comprehensively, we have probed its conformational preferences in two different solvents, DMSO-d_6 and methanol-d_4. Several families of conformers of **1** are identified, none of which correspond to the MM2* structure **2a** described previously. Comparison of the solution-derived structures with the geometric variables characterizing the NMR-bound conformation reveals a novel conformer in DMSO-d_6 that fits the NMR data with fidelity identical to that proposed by Canales et al.[12] Docking experiments shed light on the comparison, while providing a second pose[13] with potential utility for molecular design based on its compatibility with the emerging structure−activity relationship (SAR) data for the molecule.

METHODS AND RESULTS

Conformational Searching. Conformational searching was carried out with three force fields (MMFF, AMBER*, and OPLS-2005) using the mixed low-mode/Monte Carlo method[14] and the GBSA/H_2O implicit solvation model in Macromodel.[15] An energy cutoff of 10 kcal/mol was used to ensure extensive adequate conformational coverage. In each of the three searches, the global minimum was found at least 10 times, indicating that the torsional energy surface has been exhaustively sampled.[16] The conformations from each force field were further minimized to convergence using the same force field and 50 steps of full matrix Newton−Raphson optimization. Structures from the three searches were pooled, and duplicates were discarded. The resulting collection of 2053 distinct DCT conformations served as input for the NMR analysis of molecular flexibility in solution (NAMFIS) study.

A separate conformational search for DCT was performed in Maestro 8.5 using the MM3*/GBSA/H_2O force field and the mixed low-mode/Monte Carlo method.[14] After 40 000 search steps and a cutoff off 7 kcal/mol, 1956 optimized conformations were obtained. The *s-trans* DCT global minimum[5,17] was located six times. To locate the proposed binding conformation (Conf-1;[12,17] see below) in this data set, we searched the conformational pool with rapid overlay of chemical structures (ROCS)[18] employing Conf-1 as the search template. It was found as the 685th conformer with an energy of ΔE = 5.4 kcal/mol above the global minimum. This compares favorably with the 4.7 kcal/mol structure reported by Canales et al.[12] The slight difference in energy can be attributed both to the use of a different version of Maestro and to the location of a different rotamer for the C−OH bonds.

NMR Data. The NMR data for dictyostatin in methanol-d_4 were those of Paterson et al.[5] The qualitatively described NOESY signals were translated into proton−proton distances as follows: very strong 2.5, strong 2.8, medium 3.5, and weak 4.2 Å with error windows of 0.1−0.2, 0.2, 0.3, and 0.4 Å, respectively.[19,20] NMR experiments conducted in DMSO-d_6 were performed on a Bruker Avance spectrometer operating at 600 MHz and equipped with an XYZ-gradient triple resonance probe. Spectra were processed using Topspin and analyzed using the iNMR software. The sample was prepared by dissolving 1.7 mg of dictyostatin in 0.5 mL of DMSO-d_6. ^{1}H and all 2D spectra were accumulated at 298 K. Five ROESY spectra were recorded at 70, 100, 150, 180, and 200 ms mixing times to check the linearity of the cross-relaxation buildup rate. The acquisition times $t1$ and $t2$ for the ROESY experiments were 207 and 26 ms, respectively. Relaxation delay was set to 3 s, and 80 scans were accumulated per $t1$ increment.

NAMFIS Analysis. The NAMFIS methodology has been described in detail elsewhere.[19,20] It seeks to identify the "best fit" between the NMR data ($^3J_{H-H}$ and NOESY cross peaks; torsion angles and interproton distances, respectively) and a "complete" set of conformations. To accommodate the structural and energetic inconsistencies among force fields, we usually perform extensive conformational searches with three different force fields and combine all nonduplicate conformations (see Methods) to generate a "complete" set. Thus, NAMFIS accepts a pool of conformations from an exhaustive conformational search and varies the mole fraction of each of these conformers to identify an optimum combination that best fits the averaged NMR data. Thus, a least-squares fit of the calculated and experimental coupling constant values and proton−proton distances is performed for every conformer sampled against the background of the remaining structures. Goodness of fit is expressed as the sum of squares of differences (SSD)[19,20] for the final deconvoluted set of NAMFIS conformers. The lower the SSD, the better the fit to the NMR data: below 100, excellent; between 100−150, satisfactory.

Coupling Constant−Dihedral Angle Interconversion. The Karplus equation parametrized by Haasnoot, de Leeuw, and Altona[21] as incorporated in the Macromodel software[22] was used for calculation of dihedral angles from coupling constants. Given that several torsion angles ϕ from 0 to 360° are associated with a single value of $^3J_{H-H}$, we confirmed values of the J-to-ϕ angles by applying an independent in-house computer program that performs the reverse conversion for individual substituent types.[23]

Protein−Ligand Docking; Pose Generation. As a preliminary to docking, the $\alpha\beta$-tubulin dimer (PDB code 1JFF) was "prepared" in Maestro 8.5.207 (Protein Prep Wizaard) by adding

hydrogens, assigning bond orders, and optimizing bond lengths, bond angles, torsion angles, and nonbonded interactions with OPLS-2005. Modest restraints were placed on heavy atoms so that strain could be relieved without deviating significantly from the input structures. Subsequently, a standard precision (SP) rigid GLIDE (v 3.5)[24] docking was performed using both the DCT structure as derived by Canales et al. (Conf-1, see below) and a DCT structure identified by NAMFIS that is compatible with the bound structure determined by transferred nuclear Overhauser spectroscopy (TR-NOESY) NMR (Conf-2, see below). All settings for grid generation and SP docking were default. The grid was centered around the native paclitaxel ligand in 1JFF. Finally, a Prime molecular mechanics generalized Born surface area (MM-GBSA)[25] energy rescoring was performed on the top 20 GLIDE poses using default settings.

For RosettaLigand[26] docking, the Maestro-prepared tubulin dimer was reduced to the β-tubulin monomer, the paclitaxel ligand was removed, and the ligand coordinates were used to define six different starting points using standard default values. DCT was docked as a rigid body into the protein, and 1000 docking poses were analyzed to select the 20 top poses as scored by RosettaLigand. These ligand−protein poses were subjected to Prime MM-GBSA energy rescoring.

For the AutoDock[27] treatment, the Maestro-prepared $\alpha\beta$-tubulin was reduced to β-tubulin, and the PTX and guanosine triphosphate (GTP) ligands were removed. The DCT ligand and protein were imported into AutoDockTools (ADT v 1.4.5), and ADT was employed for ligand and protein preparation for compatibility with Autodock. A grid was constructed to encompass the empty paclitaxel binding site and parametrized using Autogrid4. A total of 100 docking poses was generated using Autodock4 with default settings for both Autogrid and Autodock. The 100 poses were clustered using ADT, and the lowest energy docking pose from each cluster was rescored using Prime MM-GBSA.

DISCUSSION

Cambridge−HOI NMR Coupling Constant Analysis. The first reported investigation of the solution conformations of dictyostatin proposed that the compound is characterized by a relatively rigid sector from C-2 to C-16 and a flexible segment from C-16 to C-23.[5] The NMR signals of the latter were interpreted in terms of the time averaged spectra of two interconverting conformations in which the C1−C2 lactone bond is either *s-cis* unsaturated ("lactone-in", **2b**) or *s-trans* unsaturated ("lactone-out", **2a**). Figure 2 illustrates the conformational difference. On the basis of an MM2*/GBSA/H_2O force field conformational search, the global minimum energy *s-trans* conformer **2a** was identified as an "acceptable match" with the NMR data and proposed as the dominant conformation in solution.[28] An alternative interpretation views dictyostatin with its 22-membered ring, six-carbon C-21 diene side-chain and 17−21 easily rotatable single bonds as a molecule with a considerably more complex conformational energy surface. Thus, the ambient temperature NMR spectrum of **1** can also be viewed as a fully averaged signature of a diverse family of rapidly exchanged conformational forms in which any single conformation accommodates only a fraction of the observed NMR parameters. The present work explores this interpretation.

The work was initiated by examining the proposition that dictyostatin's experimental coupling constants and those calculated from the MM2* global minimum **2a** correspond to similar structures. Surprisingly, comparison of the list[5] of experimental and calculated coupling constants indicates that there are significant discrepancies between several pairs of coupling constants, which in turn are expected to translate into substantial differences between the dihedral angles derived for the two structures. For example, the observed and calculated $^3J_{H-H}$ values for H5−H6 and H8b−H9 differ by 4.4 and 8.7 Hz, respectively. The coupling constants for H18a−H19, H19−H20, and H20−H21 are mismatched by 5.9, 4.3, and 5.0 Hz, respectively.[5] A full list of the $^3J_{H-H}$ values and dihedral angles corresponding to the calculated and experimental coupling constants is provided in the Supporting Information (Table S1). It is noteworthy that, between the two sets of data, six torsional angles differ by at least 10−20°, while 12 differ by greater than 20°.

To probe the nature of the conformation corresponding to the torsional angles derived from the measured $^3J_{H-H}$ values, we generated structure **3** corresponding to the dihedral angles derived from these coupling constants by employing the modified Karplus equation of Haasnoot, de Leeuw, and Altona.[21] Figure 2 illustrates that **3** is acyclic with a 4.9 Å gap between C2 and C3 doubly-bonded carbons that require a 1.4 Å bond distance to create a closed dictyostatin ring. In addition, a 1.6 Å steric clash between the C7-OH oxygen and the C-20 methyl carbon underscores the high-energy nature of this structure. Figure 2 reveals that structures **2a** and **3** are quite different in their overall geometries. While **3** is clearly a virtual structure,[29] it is possible that conformer **2a** is in the same category. As has been noted in previous studies, the assignment of averaged NMR data to a single conformation inevitably leads to a high energy virtual structure.[11,19,20,30]

Dictyostatin Conformations in CD_3OD. NAMFIS analysis was performed with the Cambridge−HOI NMR data set and the 2053 unique optimized conformations described in the Methods section to provide a pool of 16 conformers with estimated populations ranging from 11% to 2%.[31] Of these, the first (11%) and fourth (8%) differ only by an OH rotation, contributing a total of 19% to the conformer pool.

Given that the NMR data are not quantitative (i.e., NOESY cross-peaks were catalogued as very strong to weak), this data-to-structure fit achieves an SSD[19,20] of 150. Its significance, however, is highlighted by the fact that **2a** alone constructed with the same data delivers an SSD of 1733.[32] The NAMFIS ensemble of conformations is clearly a superior solution to the data-fitting problem. Seven of the top 16 conformations, including the top three (Figure 3), display the *s-cis* unsaturated lactone-in conformation (52% of the total ensemble). In this respect, the NAMFIS analysis agrees qualitatively with the Paterson et al. deduction[5] that there is an approximately even distribution of *s-cis* and *s-trans* unsaturated lactone forms.

This observation is at odds with the proposal that *s-trans* lactone-out **2a** is the dominant conformation in solution. The NAMFIS conformation closest to **2a** in terms of root-mean-square deviation (rmsd) is the sixth best-fit present to the extent of 7%. However, even this conformation differs substantially from the **2a** conformer in several parts of the molecule. Figure 4 shows the overlap of the two conformations with an all-atom rmsd of 2.7 Å.

As noted above, the Cambridge−HOI team not only deduced the full stereogenic assignment for **1**, but also proposed the existence of at least two rapidly equilibrating conformations in the C16−C23 region. The *s-trans* unsaturated lactone-out form (**2a**) was proposed to be more stable than the *s-cis* unsaturated lactone-in (**2b**) conformer based on relative MM2* energies. The latter relative stability prompted the identification of the MM2* *s-trans* global minimum **2a** as the dominant conformer in solution. Unfortunately, force field energies for structures as complex and polar as **1** are capricious and ordinarily difficult to correlate with experiment.[33]

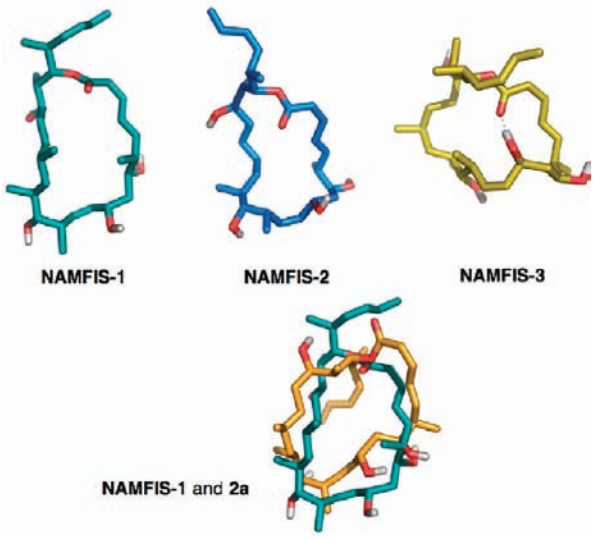

Figure 3. The three most populated NAMFIS conformers in methanol-d_4: NAMFIS-1 (11%), NAMFIS-2 (11%), and NAMFIS-3 (9%). The latter is predicted to enjoy an internal hydrogen bond. The pair below superposes **2a** (orange) with NAMFIS-1; all-atom rmsd = 4 Å.

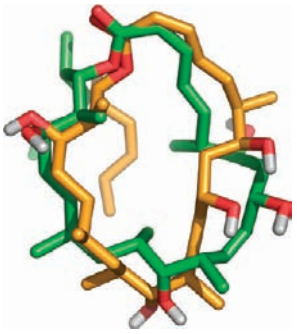

Figure 4. Heavy-atom overlap of **2a** (orange) and the most similar NAMFIS conformation in methanol-d_4 (green, sixth best-fit, 7%); rmsd = 2.7 Å.

NAMFIS, on the other hand, not only avoids the ambiguities of intuitively disentangling complex NMR spectra but also bypasses the pitfalls of attempts to predict relative energies in solution. It simultaneously eliminates the temptation to arbitrarily select a global minimum from a specific force field as an experimental conformation.[33] By extracting conformer mole fractions in solution on the basis of structure, as is the case with NAMFIS, the relative free energies can be calculated directly from the populations. In the present case, conformer **2a** is not among the ensemble of conformers derived from the methanol-d_4 data measured for **1** (cf., Figure 4 and SSD comparison). Likewise, the *s-cis*, lactone-in motif is the favored geometry posited for dictyostatin in the same solvent.

It is pertinent to ask whether the ensemble of dictyostatin conformers obtained by the NAMFIS analysis accounts for all the NMR parameters provided in the Cambridge/HOI report. This is a stringent criterion for evaluating NAMFIS performance. If any of the NMR data are not satisfied by one or more of the NAMFIS conformers, then it is likely that complete coverage of conformational space has not been achieved. Gratifyingly, the top 16 NAMFIS conformers collectively fit every piece of NMR data that is observed for both the rigid as well as the flexible portions

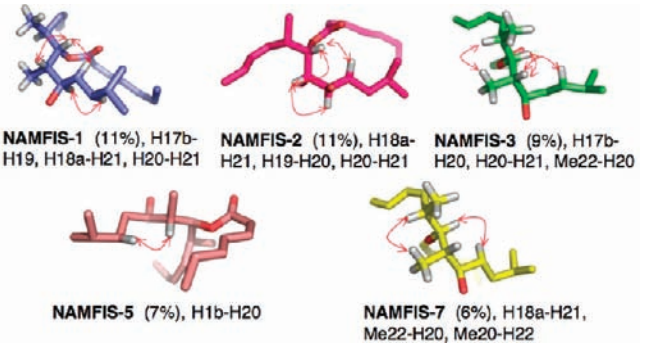

Figure 5. The shapes of the C16−C23 fragments for five NAMFIS conformers in methanol-d_4 (populations estimated to range from 6% to 11%) and the partial NOE data that they satisfy. For example, H17b−H19 corresponds to an NOE crosspeak observed between these two protons.

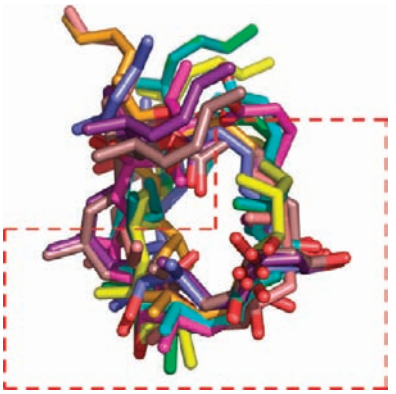

Figure 6. Superposition of the 10 most populated DCT NAMFIS conformers in methanol-d_4 by ring atoms within the C2−C16 sector (red outline). The rmsd's relative to the top ranked conformer (NAMFIS-1) range from 0.2 to 1.8 Å.

of dictyostatin. At the same time, no single conformer satisfies all the data. Significantly, for the flexible portion of the molecule (C16−C23), we find that one-half of the top conformers satisfy the NMR data for the *s-cis*, lactone-in conformation in contrast to the single **2a** *s-trans* conformer arising from MM2* energies.[5]

Figure 5 displays the flexible C16−C23 portions of the molecule for some of the top NAMFIS conformations and the NOE data that are matched. The remainder of the molecule, C2−C16, was proposed to be relatively rigid.[5] Evaluation of the NAMFIS conformers indicates that the top conformer contributes strongly to the NMR data in the C10−C16 region, but, like the remaining 15 members of the NAMFIS pool, accounts for structural features within C2−C16 and other sectors to limited and various extents.

The conclusion that dictyostatin is relatively rigid in the C2−C16 fragment would be premature. There are many conformations associated with the C2−C16 fragment that can contribute to a fit of the NOE/$^3J_{H-H}$ data. Figure 6, superposing C2−C16 for the second to tenth most populated NAMFIS structures on the most populated NAMFIS-1, makes it clear that this segment of **1** cannot be regarded as even relatively rigid. The molecule is characterized by a spread of conformations. The rmsd's for ring carbons of NAMFIS-2 to NAMFIS-10 relative to NAMFIS-1 in the C2−16 region range from 0.2 Å for the fourth ranked conformer (virtually identical) to 1.8 Å for the tenth

dx.doi.org/10.1021/ja1023817 |*J. Am. Chem. Soc.* 2011, 133, 2427–2436

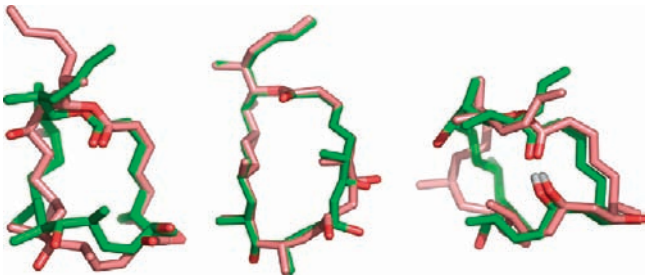

Figure 7. Superpositions of similar conformations found in DMSO-d_6 (green) and methanol-d_4 (pink); from left: DMSO-1 (20%) and methanol-2 (11%) (rmsd 2.3 Å), DMSO-3 (10%) and methanol-1 (11%) (rmsd 1.6 Å), and DMSO-2 (13%) and methanol-3 (9%) (rmsd 1.8 Å).

ranked conformation. Thus, all 16 NAMFIS conformers contribute intensity to the NOE cross-peaks and $^3J_{H-H}$ values, observations that suggest relative rigidity when analyzed only as one or two conformers.

Comparison of Dictyostatin Conformations in Methanol and DMSO. To perform a dictyostatin conformational analysis based on more quantitative data and to investigate solvent effects, we examined the NMR spectra for **1** in DMSO-d_6. A total of 35 NOE distances and 15 $^3J_{H-H}$ values were extracted from the averaged NMR spectrum. When processed by NAMFIS, the DMSO-based quantities gave 15 conformations ranging from 1% to 20% populations. The previously described two MM2 conformations are again absent from the conformational ensemble. Within the 15 conformations, only three present the unsaturated lactone *s-trans*, while all others, including the top three, exhibit the unsaturated lactone *s-cis*. Thus, the *s-cis* form is even more dominant in DMSO-d_6 than in methanol. Intramolecular hydrogen bonding among the confomers is also consistent with the nature of the solvent: 46% of the conformers are internally hydrogen-bonded in DMSO-d_6, although only 18% are hydrogen-bonded in methanol. This agrees with DMSO's ability to accept hydrogen bonds,[34] while methanol both donates and accepts them.

Close inspection of the conformational profiles in the two solvents reveals certain common features. Thus, some conformations in the two media are very similar, but with differing populations. For example, the best-fit DMSO-d_6 conformation is similar to the second best-fit methanol conformation, while the third best-fit DMSO-d_6 conformation is similar to the best-fit methanol conformation. The top DMSO-d_6 conformation (20%) is identical to the ninth best-fit methanol-d_4 conformation (5%). These similarities are illustrated in Figure 7 and indicate that solvent properties promote a redistribution of the equilibrium among conformational families in solution without altering the fundamental nature of the conformations themselves.

Clustering of dictyostatin conformations by inspection and using the superposition tool in Maestro (v 8.5) allows classification into five dominant families as illustrated by Figure 8. These are the Crescent, Extended, Open, Compact, and Other forms. Of these, the Crescent family dominates in both DMSO-d_6 and methanol (44% and 45%, respectively) with the Extended family being the second-most dominant form in methanol (23%) and third-most dominant geometry in DMSO-d_6 (19%). The Extended family is also represented among the top five conformations in both solvents. The Open family is present only in methanol (14%) as the third-most dominant family, while the Compact family is the second-most dominant in DMSO-d_6 (21%) and fourth-most dominant in methanol (4%). Conformations from the Other families are present to the extent of 13% and 8% in methanol and DMSO-d_6, respectively. While features of the latter conformers cannot be completely ascribed to any one of the other families, they share partial structural elements with other family members. The two MM2* conformations discussed above, while not found in either methanol-d_4 or DMSO-d_6 in the present study, belong to the Compact family.

Observation of similar conformational ensembles in both solvents further reinforces the commonality of conformations with modified populations caused by solvent effects.

Dictyostatin Conformations in the β-Tubulin Taxane Binding Pocket. A proposal for the tubulin-bound geometry of dictyostatin has recently been deduced by means of transfer-NOESY NMR evaluation. The structure was identified as a MM3*/GBSA molecular mechanics minimum by conformational searching. Neither the *s-trans* global minimum[5] nor the lowest energy *s-cis* form (ΔE = 2.0 kcal/mol) provide a satisfactory fit to the NOE-distance and ^3J-determined torsion angles. However, the geometry of a third local MM3* minimum (Conf-1, ΔE = 4.7 kcal/mol) furnished a satisfactory match to the NMR parameters.[12]

Previous work has shown that conformations present in solution, often with low mole fraction, correspond to the protein-bound form.[35,36] Consequently, we have mapped the TR-NOESY quantities for the bound ligand reported by Canales and colleagues[12] onto the NAMFIS conformations of DCT in DMSO-d_6 and methanol-d_4. All unique conformers deliver SSDs exceeding 400 (see Methods) except for the seventh best-fit conformer in DMSO-d_6 (7%, Conf-2 (NAMFIS-7)) with an SSD = 122. This structure belongs to the same family as the Canales et al. conformation, although the two structures differ especially in the C6−C18 region (Figure 9). For comparison with Conf-2, Conf-1[12] was fitted to its own NMR data using NAMFIS to deliver an SSD of 127. Although the two conformations are of equal quality from the point of view of TR-NOESY-determined molecular geometry, they differ in energetic characteristics. Because Conf-2 is present in DMSO-d_6 (but not methanol-d_4), the populations listed in Table S1 can be converted into relative free energies by applying the Boltzmann

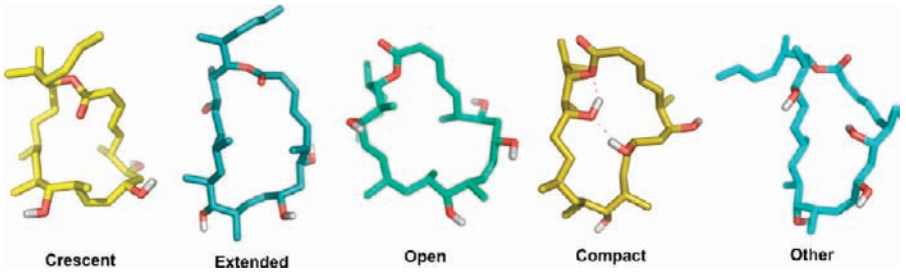

Figure 8. The five dictyostatin families present in DMSO-d_6 and methanol-d_4.

dx.doi.org/10.1021/ja1023817 |J. Am. Chem. Soc. 2011, 133, 2427–2436

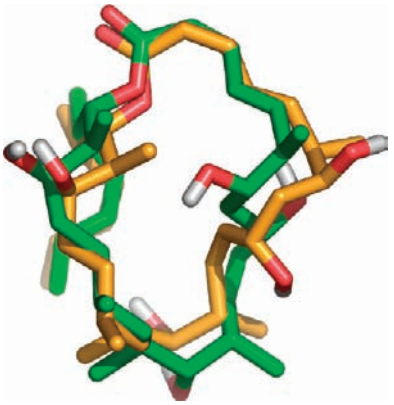

Figure 9. Heavy atom superposition of TR-NOESY dictyostatin conformers Conf-1 (green) and Conf-2 (DMSO-7, gold); rmsd = 1.6 Å.

equation. The 7% populated conformer resides ΔG = 0.6 kcal/mol above the global minimum in this medium. At this energy, it is both a structurally and an energetically suitable candidate for binding to tubulin. Because Conf-1 appears in neither of the two solvents, it is not possible to derive a comparable free energy estimate. The ΔE = 4.5−5.5 kcal/mol MM3*/GBSA/H_2O molecular mechanics relative strain energy (see Methods) is not indicative of the solution state because it represents an entirely different energy scale that is dependent on force field parametrization and atomic charge assignments.[33]

To further probe the nature of these conformations, rigid docking of both Conf-1 and Conf-2 into the taxane binding pocket of β-tubulin was performed utilizing Glide,[24] RosettaLigand,[26] and AUTODOCK (v 4.0).[27] The latter two docking methods explore the flexibility of the side-chains within the binding site. The refined electron crystallographic protein coordinates of the tubulin dimer (PDB code 1JFF) served as ligand receptor here and in the previous Canales et al. study to rationalize the NMR-derived interatomic proton−proton separations of the bound conformation. Because docking scores from different methods arise from separate and streamlined scoring functions, subsequent MM-GBSA rescoring was carried out to improve conformer discrimination and to standardize the results. The MM-GBSA protocol has been shown to be an effective tool for ordering docked poses[13] in good agreement with experimental structure determination.[25]

The Canales et al. TR-NOESY-derived conformation for DCT (Conf-1) was rigidly docked into the taxane binding pocket of β-tubulin with each of the three docking programs and subsequently rescored by MM-GBSA. The results indicated a high degree of ambiguity, because Conf-1 can adopt a number of poses without sacrificing substantial binding score energy. Thus, the most favorable binding pose of three identified by AUTODOCK gave a final relative ΔG value of −30.3 kcal/mol (Pose-1c). The latter was followed by a RosettaLigand binding pose at −28.5 (Pose-1b) and the original Canales et al.[12] AUTODOCK pose (Pose-1a) scoring −26.5 kcal/mol (Figure 10). What is the source of the discrepancy between this ranking and the latter previously derived AUTODOCK pose? Because the MM-GBSA protocol has been used to rescore poses within and across several docking methods, it would appear that the earlier AUTODOCK Conf-1a complex[12] is less favored relative to other poses on the more elaborate MM-GBSA energy surface. Nonetheless, given the assumptions embedded in the docking methods and the resolution of

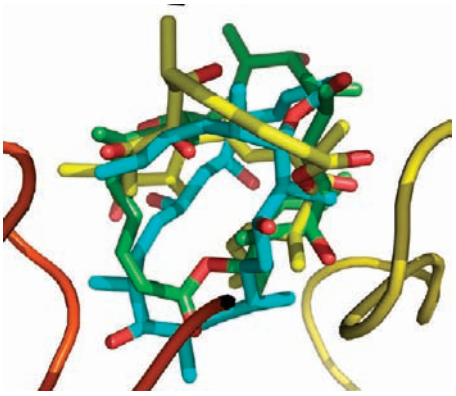

Figure 10. The three most favorable docking poses[13] of Conf-1 in β-tubulin: green (AUTODOCK (Canales et al.)[12] −26.5, Pose-1a), yellow (RosettaLigand, −28.5, Pose-1b), blue (AUTODOCK, −30.3 kcal/mol; Pose-1c).

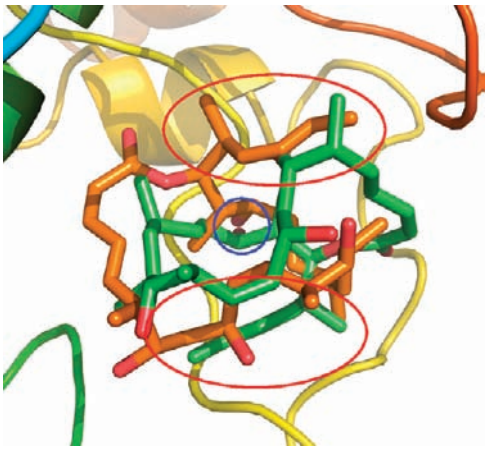

Figure 11. Superposition of two poses[13] of DCT in β-tubulin: Pose-1a/Conf-1 (green) and Pose-2/Conf-2 (orange). Opposing dienes reside inside the red ovals, while C19−O is surrounded by the blue circle.

the 1JFF protein (3.5 Å), we regard these different poses as equally likely candidates for the DCT−tubulin complex.

In contrast to the promiscuous binding of Conf-1, Conf-2 (DMSO-7/NAMFIS) provided a single dominant binding pose with a relative ΔG value of −33.6 kcal/mol. This pose (Pose 2), produced by both Glide and AUTODOCK, shows some spatial features that resemble those of the Conf-1c (−30.3 kcal/mol) binding mode (see Figure S1). Interestingly, the original Canales et al. pose (Conf-1a, Figure 10, blue) and the present best-scored pose (Conf-2) are "flipped" poses of one another, the structures rotated approximately 180° around an axis through the C19−O bond (Figure 11). For the Conf-2 pose, a hydrogen bond between C19−OH and the C═O of Pro274 on the M-loop is evident. The top scoring AUTODOCK Conf-1c pose also displays this hydrogen bond, prompting the idea that Pro274 might be a strategically important amino acid for DCT because the M-loop is a critical element for maintaining the protein−protein interface between tubulin protofilaments in microtubules.

SAR of Dictyostatin from Ligand Conformation and Tubulin Binding Models. To further try to discriminate possible binding modes for DCT, we examined aspects of the molecule's emerging SAR. Two studies have reported that saturation of the

dx.doi.org/10.1021/ja1023817 |J. Am. Chem. Soc. 2011, 133, 2427–2436

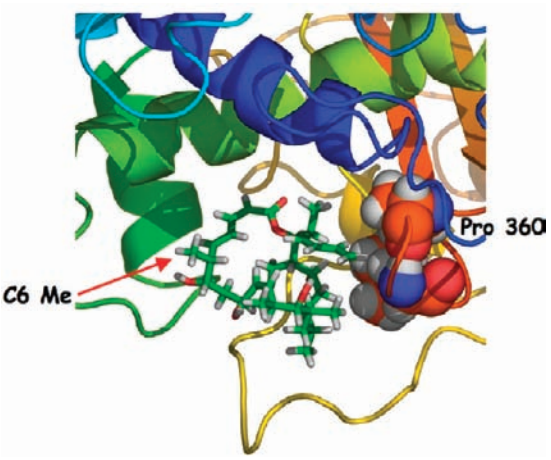

Figure 12. The DCT Pose-2/Conf-2 (DMSO-7) in the taxane binding pocket of tubulin as derived by Glide and AUTODOCK. The C6 methyl group is not in contact with the protein, solvent exposed.

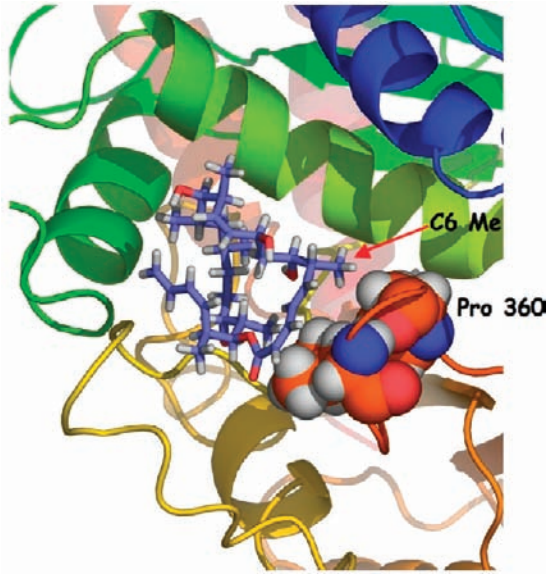

Figure 13. The Canales et al. Pose-1a/Conf-1 DCT pose in the taxane binding pocket illustrating the close contact of C6 methyl and Pro360.

C2−C5 diene moiety and elimination of the C6 methyl leads to trivial loss of activity.[3g,37] In addition, 6-epi dictyostatin has been demonstrated to have a potent effect on tumor growth that is equivalent to DCT itself.[38] Accordingly, these observations have suggested that the C2−C6 sector of the molecule may not be in close proximity to the protein and, therefore, amenable to synthetic manipulation without sacrificing microtubule stabilizing potency.

Inspection of Pose 2 (Conf-2) reveals that one face of the C2−C6 fragment resides above a hydrophobic pocket formed by Leu217, Leu230, and Leu275, while the other face is exposed to solvent. The latter applies to the C6 methyl as well, the closest protein side-chain being His229 (Figure 12). This DCT orientation is consistent with the weak involvement of this region in mediating protein−ligand interactions. In contrast, the NMR-based Pose 1a (Conf-1) places its C2−C6 molecular sector within van der Waals contact of the nonpolar side-chains of Leu 371 and Pro 360 (Figure 13). Particularly interesting is the 2.9 Å H---H van der Waals contact between the C6 methyl group and Pro360, an interaction that is expected to reduce activity if the methyl is eliminated.

Synthetic inversion of the C9 hydroxyl causes significant loss in activity, while capping the hydroxyl with a methyl group to give 9-methoxy DCT causes no noticeable change in growth inhibition across a range of cell lines.[39] In both models, methylation of the C9−OH followed by binding site optimization resulted in no additional ligand−protein contacts, implying that both models can accommodate a methoxy group at this position. However, inversion of C9−OH in Pose-2 delivers potential intramolecular steric crowding by effecting a modest clash between C9−OH and one of the C15 protons. The same operation for Pose-1a causes no discernible steric clashes and in fact leads to proximity of the hydroxyl proton to the nitrogen of a His229 with which it can potentially form a hydrogen bond. Thus, the reduction in activity associated with C9 inversion seems to be more consistent with Pose-2.

The preferred configuration of C19−OH is *R*, with inversion leading to a loss in potency in a series of biological tests.[3g] In the Conf-1/Pose-1a model, this OH group forms hydrogen bonds with the Pro274 backbone carbonyl and the Thr276 NH. Hydroxyl inversion followed by optimization of the modified DCT structure leads to switching of this hydrogen bond to the Thr276 backbone carbonyl, causing no specific hindrance to adoption of this new pose. Similarly, the same C19 *R* configuration in the best docked Conf-2 pose engages in a hydrogen bond with the Pro274 backbone carbonyl. In this case, however, inversion of the hydroxyl followed by binding site optimization leads to steric congestion between the hydroxyl oxygen and the C21 and C23 protons (O---H distances 2.5 Å). Thus, this pose appears to be disfavored, consistent with the loss of potency.

A remarkable SAR diagnostic for dictyostatin concerns the observation that both the natural C16−Me DCT and the corresponding normethyl analogue cause similar growth inhibition for 1A9 cells, but the 1A9/PTX mutant cell line exhibits 1000-fold resistance to the normethyl compounds. The mutant tubulin involves transformation of Phe270 to Val270.[3g,40] The drastic reduction in activity for the C16 methyl-depleted DCT toward the mutant has been interpreted as implying a potency-enhancing proximity of the C16−Me group to the Phe270 aromatic ring or the Val270 isopropyl group in the wild-type and mutant proteins, respectively. The loss of such an interaction by methyl deletion is tolerated by wild-type, but not mutant protein. This enigma is most likely complicated by the presence of a "hole" in the mutant protein followed by differential water occupation depending on the nature of the bound ligand. It is noteworthy that removal of the methyl group is tolerated only by the wild-type tubulin. Inspection of the two poses (Figures 12 and 13) reveals that in both cases the C16−Me group is not in proximity to Phe270. In Pose 1a, the carbon atom of the methyl group is situated at a distance of 5.5 Å from the nearest carbon of the Phe270 phenyl ring, while in Pose 2 it resides near Gln282. A simple interpretation of the resistance in terms of the latter pose can be formulated.

As illustrated by Figure 14, the C16 and C22 methyl groups are situated at opposite ends of the Conf-2/Pose-2 structure. The C16−Me engages in a hydrophobic interaction with the methylenes of the side-chain of Gln282 (H---H, 2.5 Å), while C22−Me beneath the phenyl ring of Phe272 likewise enjoys a hydrophobic contact. If the C16−Me is removed and simultaneously the Phe272 is truncated to Val272, two "holes" are created in the

dx.doi.org/10.1021/ja1023817 |*J. Am. Chem. Soc.* 2011, 133, 2427–2436

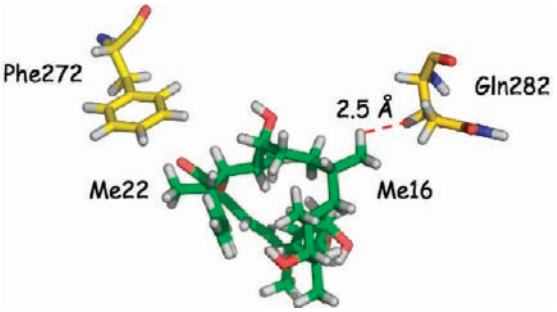

Figure 14. DCT Pose-2/Conf-2 illustrating the location of Me22 near Phe272 and Me16 near Gln282 in the tubulin−taxane binding site.

binding pocket. It is plausible that both sites fill with water, compete with the ligand,[41] and either drive the normethyl analog out of the mutated binding site or prevent it from tight association. In Pose-1a, similar factors might also operate, but because the C16−Me group and Phe270 occupy the same pocket subsite, simultaneous methyl removal and mutation of Phe to a Val would only create one cavity as opposed to two. To be sure, water-soaking and the entropy associated with water migration might likewise result in expulsion of normethyl DCT in such a scheme as well. In this interpretation, the wild-type tubulin permits little or no access to water molecules for either DCT or its normethyl analogue. It would appear that the balance is tipped, however, when a relatively large cavity on the hydrophobic floor or the binding site is generated by the Phe to Val side-chain truncation. A similar effect obviously operates for PTX, which experiences a 25-fold resistance by 1A9/PTX cell relative to wild-type. In that situation, a tight phenyl−phenyl contact is perturbed when a gap opens between the C13 PTX phenyl ring and the smaller valine.

On the Possibility for Multiple DCT Binding Modes. A reviewer has commented that because the expansive tubulin binding site is bounded by loops (i.e., linking H6−H7, B7−H9 (M-loop), and B9−H10), this region of the protein might be particularly flexible and capable of supporting multiple binding modes[42] for the DCT ligand. To address this issue, we have performed three numerical experiments. The first examines protein flexibility by reanalysis of a 10 ns MD simulation performed with GROMACS 3.2.1 for the PTX-free α,β-tubulin dimer (PDB code 1JFF) solvated in a box of 35 000−39 000 SPC water molecules and complemented by two Mg^{2+} and 36 Na^{+} at 300 K.[43] The largest motion resides in the reorganization of the M-loop (Phe275−Val283) with an average rmsd of ∼8 Å relative to the 1JFF starting point as described previously.[44] In particular, the M-loop in the 1JFF starting structure is located away from the taxane binding site consistent with providing access for incoming or departing ligands. Over the 10 ns trajectory, the open binding site is occluded by the collapse of the M-loop, which is essentially complete at 2.5 ns. Figure 15 illustrates the movement both with and without the DCT ligand.

The remaining 7.5 ns leads to variations in loop conformation and side-chain reorganization, but at no point is access to ligands permitted. During the initial 2.5 ns, the B9−B10 loop (358−362) shifts in concert with the M-loop accommodating its capping of the taxoid binding site (average rmsd of ∼4 Å, Figure 15). By contrast, the loop bridging the H6−H7 helices is relatively stable. The flexibility of the binding pocket expresses itself during the first 2.5 ns of dynamics. Side-chains at the bottom of the pocket are relatively unchanged, while those at the top of the site experience the greatest movements, again in concert with M-loop

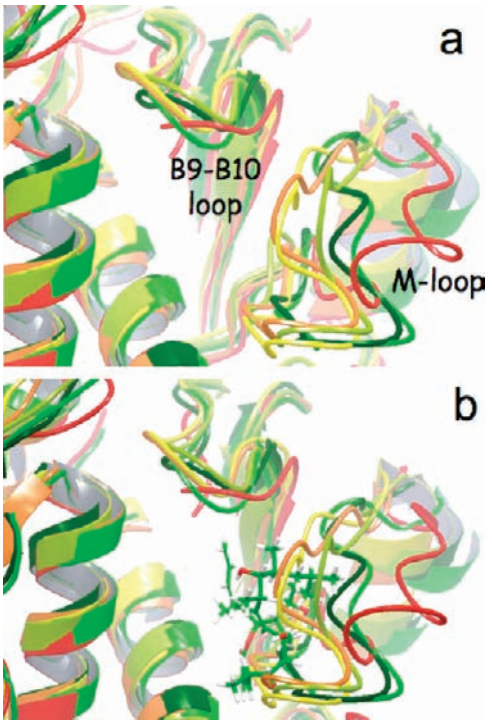

Figure 15. Superposition of the β-tubulin binding sites for the 6 MD time-points: 0 (original (1JFF), red), 250 (dark green), 750 (green), 1250 (yellow green), 1750 (yellow), and 2000 ps (orange); (a) superposed proteins for the 6 MD time-points (0−2000 ps); (b) superposed proteins with 6 time-points (0−2000 ps). Pose-2/Conf-2 (Figure 12) is located in 1JFF (0 ps, red). Note the movement of the M-loop over the binding site from red to orange.

reorganization. For example, the Arg282 backbone carbonyl (M-loop middle) displays significant displacement during this time-course. A series of trajectory plots found in the Supporting Information illustrates the changes. With respect to reshaping the binding pocket to allow multiple binding modes for DCT, we followed the trajectories of three M-loop amino acids in contact with the ligand in the two preferred binding models: Pro272, Leu273, and Thr274. Because these side-chains undergo significant movement early in the M-loop translations (see the Supporting Information), loop repositioning in response to ligand shape[43] has the potential to accommodate multiple binding modes. On the other hand, the next numerical experiments are interpreted to rule it out.

Second, the 10 ns MD trajectory for tubulin described above was examined for generation of a novel binding mode. The first 2 ns exposes the taxane binding pocket to entry by an external ligand, while the final 7.5 ns causes the pocket to experience cleft-capping by the M-loop. For this reason, snapshots of the α,β-tubulin heterodimer at 250, 750, 1250, 1750, and 2000 ps were extracted from the trajectory, and each was subjected to local refinement with Protein Prep Wizard in Maestro (see Methods: Protein−Ligand Docking) followed by rigid Glide docking of Conf-2 into the taxoid binding site. The 10 lowest energy Glide poses for each β-tubulin time point were rescored with MM-GBSA leading to energy differences of 18.4, 10.0, 32.0, 24.8, and 25.1 kcal/mol relative to Pose-2/Conf-2 (Figure 12). The best pose at 750 ps is estimated to be 10 kcal/mol higher than the latter. Each of the five Conf-2 liganded trajectory structures was also visually analyzed for consistency with the SAR described in

the previous section. In particular, the C2−C5 diene, C6−Me, C9−OH, and C16−Me moieties were examined. No single Conf-2/β-tubulin MD complex accommodates the SAR without violating at least one of the SAR conditions. In summary, we conclude that none of the MD time-point structures provide a novel binding mode based on both relative MM-GBSA energies and SAR analysis.

Third, a NAMFIS fit of the 13 DMSO conformers to the NMR data for the Canales et al. bound form of DCT was carried out to probe whether multiple conformations from this pool could explain the data better than the single NAMFIS-7 conformer. Indeed, 5 of the 13 conformers collectively deliver an SSD of 85 as compared to the single conformer SSD value of 127. Gratifyingly, the top conformer was NAMFIS-7 (Conf-2), contributing 54% to the solution. To examine the possible role of the other four conformers (46%), we Glide-docked each into the tubulin binding pocket and subjected the DCT−tubulin complexes to MM-GBSA rescoring similar to that described above. The top three conformers (NAMFIS-5, NAMFIS-7, and NAMFIS-9) ranked within an 0.5 kcal/mol window. Thus, on an energy basis alone, all three can be considered as equivalent docking solutions. However, unlike NAMFIS-7, neither NAMFIS-5 nor NAMFIS-9 satisfies crucial SAR criteria for DCT binding. In the case of NAMFIS-5, neither C9−OH methylation nor C9-inversion led to discernible steric clashes or loss of hydrogen bonds, observations inconsistent with the observed loss of activity for the modified DCT analogues. The situation for NAMFIS-9 is similar. In this case, the C9 and C19 hydroxyls are intramolecularly hydrogen-bonded to one another and the C19−OH sustains a hydrogen bond with Thr276 in the M-loop. Nonetheless, inversion of C9−OH followed by energetic optimization remarkably preserves the C9−C19 hydrogen bond. This observation is at odds with the SAR profile illustrating significant loss of activity upon C9 inversion. Thus, while NAMFIS-5 and NAMFIS-9 are mathematically valid components of the NAMFIS treatment of the TR-NOESY NMR quantities and also structures delivering competitive MM-GBSA scores, their failure to comprehensively satisfy the SAR data appears to preclude them in favor of NAMFIS-7. Likewise, the remaining three conformers (NAMFIS-3, -4, and -8) all fail to satisfy relevant SAR diagnostics as well as ranking at least 4 kcal/mol higher in energy than NAMFIS-7. Thus, both energetic and functional criteria appear to reject these structures as ligands competitive with NAMFIS-7 (Conf-2) binding.

SUMMARY AND CONCLUSIONS

In summary, we have performed an empirical conformational analysis of dictyostatin in two solvents, DMSO-d_6 and methanol-d_4, using the NAMFIS methodology. Examination of the conformational profiles points to the presence of common families of rotamers with differing populations. Interestingly, the previously proposed pair of dominant methanol conformations is not among them. Reanalysis of the TR-NOESY NMR parameters for tubulin-bound DCT gathered by Canales et al. reveals a new conformation that accommodates the NMR geometry as well as the previously proposed structure. An attractive feature of this rotational isomer (DMSO-7) is that it is found in DMSO-d_6 solution as a minor contributor to the conformational equilibrium (7%), while simultaneously docking into the taxane cleft of β-tubulin in a consistent and satisfying manner. The conformation (Pose-2/Conf-2) reveals a competitive binding pose distinctly different from the Canales et al. proposal[12] (Pose-1a/Conf-1) and compatible with key aspects of the emerging SAR for this potential anticancer molecule. Several attempts to identify multiple binding modes were made, but the current models support a single binding mode. Synthetic modifications to DCT based on the two proposals can be expected to lead to compounds that further clarify mechanistic and structural features of the DCT−tubulin association, while providing valuable improvements to potency, selectivity, and the anticipated resistance.

ASSOCIATED CONTENT

Supporting Information. Tables of calculated coupling constants, torsional angles, Boltzmann populations, and relative energies for DCT conformations; conformational superpositions; and trajectory profiles for structural sectors of β-tubulin across a 10 ns molecular dynamics evaluation. This material is available free of charge via the Internet at http://pubs.acs.org.

AUTHOR INFORMATION

Corresponding Author
jsnyder@emory.edu; curran@pitt.edu

ACKNOWLEDGMENT

We are grateful to Professors Fernando Díaz and Jesús Jimenéz-Barbero (CIB-CSIC, Madrid, Spain) for sharing the coordinates of DCT bound to β-tubulin in Pose-1c (Figures 10, 11, and 13) and to OpenEye Scientific Software (Santa Fe, NM) for the generous provision of a no-cost license for the ROCS software. We are likewise appreciative of Giuseppe Balacco (iNMR) for assistance in integrating and analyzing the DCT NOESY spectrum, Pieter B. Burger (South African exchange fellow) for coordinate interconversion, Billy W. Day (University of Pittsburgh) for helpful discussion, and Professor Dennis C. Liotta (Emory University) for encouragement and support.

REFERENCES

(1) Madiraju, C.; Edler, M. C.; Hamel, E.; Raccor, B. S.; Balachandran, R.; Zhu, G.; Giuliano, K. A.; Vogt, A.; Shin, Y.; Fournier, J. H.; Fukui, Y.; Bruckner, A. M.; Curran, D. P.; Day, B. W. *Biochemistry* **2005**, *44*, 15053–15063.

(2) Mita, A.; Lockhart, A. C.; Alland, L.; Chen, T.; Bochinski, K.; Curtright, J.; Cooper, W.; Hammond, L.; Moricz, M.; Phillips, P.; Taccard, G.; Sharma, S.; Rowinsky, E.; Rothenberg, M. *J. Clin. Oncol.* **2004**, *22*, 2025.

(3) (a) Shin, Y.; Choy, N.; Turner, T. R.; Balachandran, R.; Madiraju, C.; Day, B. W.; Curran, D. P. *Org. Lett.* **2002**, *4*, 4443–4446. (b) Shin, Y.; Fournier, J. H.; Fukui, Y.; Brückner, A. M.; Curran, D. P. *Angew. Chem., Int. Ed.* **2004**, *43*, 4634–4637. (c) Paterson, I.; Britton, R.; Delgado, O.; Meyer, A.; Poullennec, K. G. *Angew. Chem., Int. Ed.* **2004**, *43*, 4629–4633. (d) O'Neil, G. W.; Philips, A. J. *J. Am. Chem. Soc.* **2006**, *128*, 5340–5341. (e) Fukui, Y.; Brückner, A. M.; Shin, Y.; Balachandran, R.; Day, B. W.; Curran, D. P. *Org. Lett.* **2006**, *19*, 301–304. (f) Ramachandran, P. V.; Srivastava, A.; Hazra, D. *Org. Lett.* **2007**, *9*, 157–160. (g) Jung, W. H.; Harrison, C.; Shin, Y.; Fournier, J. H.; Balachandran, R.; Raccor, B. S.; Sikorski, R. P.; Vogt, A.; Curran, D. P.; Day, B. W. *J. Med. Chem.* **2007**, *50*, 2951–2966. (h) Paterson, I.; Naylor, G. J.; Fujita, T.; Guzmán, E.; Wright, A. E. *Chem. Commun.* **2010**, *46*, 261–263.

(4) Matsumori, N.; Kaneno, D.; Murata, M.; Nakamura, H.; Tachibana, K. *J. Org. Chem.* **1999**, *64*, 866–876.

(5) Paterson, I.; Britton, R.; Delgado, O.; Wright, A. *Chem. Commun.* **2004**, 632–633.

(6) Florence, G. J.; Gardner, N. M.; Paterson, I. *Nat. Prod. Rep.* **2008**, *25*, 342–375.
(7) Paterson, I.; Gardner, N. M.; Poullennec, K. G.; Wright, A. E. *Nat. Prod.* **2008**, *71*, 364–369.
(8) Sanchez-Pedregal, V. S.; Kubicek, K.; Meiler, J.; Lyothier, I.; Paterson, I.; Carlomagno, T. *Angew. Chem.* **2006**, *45*, 7388–7394.
(9) Jogalekar, A. S.; Kriel, F. H.; Shi, Q.; Cornett, B.; Cicero, D.; Snyder, J. P. *J. Med. Chem.* **2010**, *53*, 155–165.
(10) Khrapunovich-Baine, M.; Menon, V.; Verdieer-Pinard, P.; Smith, A. B., III; Angeletti, R. H.; Fiser, A.; Horwitz, S. B.; Xiao, H. *Biochemistry* **2009**, *48*, 11664–11677.
(11) Kingston, D. G. I.; Bane, S.; Snyder, J. P. *Cell Cycle* **2005**, *4*, 279–289.
(12) Canales, A.; Matesanz, R.; Gardner, N. M.; Andreu, J. M.; Paterson, I.; Diaz, J. F.; Jiménez-Barbero, J. *Chem.-Eur. J.* **2008**, *14*, 7557–7569.
(13) The term "pose" refers to both the ligand conformation and its orientation in a protein binding site. Thus, Figure 11 displays two separate poses for DCT.
(14) Kolossváry, I.; Guida, W. C. *J. Am. Chem. Soc.* **1996**, *118*, 5011–5019.
(15) Still, W. C.; Tempczyk, A.; Hawley, R.; Hendrickson, T. *J. Am. Chem. Soc.* **1990**, *112*, 6127–6129.
(16) Chang, G.; Guida, W. C.; Still, W. C. *J. Am. Chem. Soc.* **1989**, *111*, 4379–4386.
(17) The PDB coordinates of DCT docked into β-tubulin and proposed as a candidate for the binding pose were generously provided by Professors Diaz and Jiménez-Barbero.[12]
(18) (a) Grant, J. A.; Gallardo, M. A.; Pickup, B. T. *J. Comput. Chem.* **1996**, *17*, 1653–1666. (b) Rush, T. S., III; Grant, J. A.; Mosyak, L.; Nicholls, A. *J. Med. Chem.* **2005**, *48*, 1489–1495.
(19) Cicero, D. O.; Barbato, G.; Bazzo, R. *J. Am. Chem. Soc.* **1995**, *117*, 1027–1033.
(20) Nevins, N.; Cicero, D. O.; Snyder, J. P. *J. Org. Chem.* **1999**, *64*, 3979–3986.
(21) Haasnoot, C. A. G.; de Leeuw, F. A. A. M.; Altona, C. *Tetrahedron* **1980**, *36*, 2783–2792.
(22) Macromodel v. 7.2: Mohamadi, F.; Richards, N. G. J.; Guida, W. C.; Lipton, M.; Liskamp, R.; Chang, G.; Hendrickson, T.; Still, W. C. *J. Comput. Chem.* **1990**, *11*, 440–467.
(23) Zhong S.; Snyder, J. P., unpublished.
(24) (a) Friesner, R. A.; Banks, J. L.; Murphy, R. B.; Halgren, T. A.; Klicic, J. J.; Mainz, D. T.; Repasky, M. P.; Knoll, E. H.; Shaw, D. E.; Shelley, M.; Perry, J. K.; Sander, L. C.; Shenkin, P. S. *J. Med. Chem.* **2004**, *47*, 1739–1749. (b) Halgren, T. A.; Murphy, R. B.; Friesner, R. A.; Beard, H. S.; Frye, L. L.; Pollard, W. T.; Banks, J. L. *J. Med. Chem.* **2004**, *47*, 1750–1759.
(25) (a) Niu, H.; Kalyanaraman, C.; Irwin, J. J.; Jacobson, M. P. *J. Chem. Inf. Model.* **2006**, *46*, 243–253. (b) Lyne, P. D.; Lamb, M. L.; Saeh, J. C. *J. Med. Chem.* **2006**, *49*, 4805–4808. (c) Graves, A. P.; Shivakumar, D. M.; Boyce1, S. E.; Jacobson, M. P.; Case, D. A.; Shoichet, B. K. *J. Mol. Biol.* **2008**, *377*, 914–934.
(26) Davis, I. W.; Baker, D. *J. Mol. Biol.* **2009**, *385*, 381–392.
(27) (a) Morris, G. M.; Goodsell, D. S.; Halliday, R. S.; Huey, R.; Hart, W. E.; Belew, R. K.; Olson, A. J. *J. Comput. Chem.* **1998**, *19*, 1639–1662. (b) Huey, R.; Morris, G. M.; Olson, A. J.; Goodsell, D. S. *J. Comput. Chem.* **2007**, *28*, 1145–1152.
(28) Global minimum (GM) energy conformers are force field-dependent, as demonstrated by the fact that the MM2* global minimum **2a** is different from the GM obtained by similar dictyostatin searches using AMBER*, OPLS, and MMFF force fields; see Methods.
(29) By "virtual structure" we mean a 3D structure that may accommodate all or a subset of the measured NMR quantities, but does not correspond to an energy minimum on either an empirical or a computational energy surface.
(30) Snyder, J. P.; Lakdawala, A. S.; Kelso, M. J. *J. Am. Chem. Soc.* **2003**, *125*, 632–633.
(31) Dictyostatin conformations can be obtained in pdb format upon request.
(32) Repeating the Cambridge-HOI MM2*/GABA/H_2O conformational search provided **2a** as the global minimum and **2b** as the second and only conformational family within 2.0 kca/mol of the global minimum. An attempt to fit these two conformations to the NMR data led to an SSD = 1096. Satisfactory fits of the NMR data usually provide SSD values below 100−150.
(33) Lakdawala, A.; Wang, M.; Nevins, N.; Liotta, D. C.; Rusinska-Rosak, D.; Lozynski, M.; Snyder, J. P. 2001; http://www.biomedcentral.com/1472-6769/1/2.
(34) (a) Kondo, M. *Bull. Chem. Soc. Jpn.* **1979**, *52*, 521–523. (b) Nazir, H.; Yildiz, M.; Tahir, M. N.; Uikü, D. *J. Mol. Struct.* **2000**, *524*, 241–250. (c) Crisp, G. T.; Jiang, Y.-L. *Arkivoc* **2001**, *vii*, 77–87. (d) Ko, H.; Shim, G.; Kim, Y. *Bull. Korean Chem. Soc.* **2005**, *26*, 2001–2006.
(35) (a) Snyder, J. P.; Nettles, J. H.; Cornett, B.; Downing, K. H.; Nogales, E. *Proc. Natl. Acad. Sci. U.S.A.* **2001**, *98*, 5312–5316. (b) Ganesh, T.; Guza, R. C.; Bane, S.; Ravindra, R.; Shanker, N.; Lakdawala, A. S.; Snyder, J. P.; Kingston, D. G. I. *Proc. Natl. Acad. Sci. U.S.A.* **2004**, *101*, 10006–10011.
(36) Thepchatri, P.; Eliseo, T.; Cicero, D. O.; Myles, D.; Snyder, J. P. *J. Am. Chem. Soc.* **2007**, *129*, 3127–3134.
(37) Paterson, I.; Gardner, N. M.; Guzmán, E.; Wright, A. E. *Bioorg. Med. Chem.* **2009**, *17*, 2282–2289.
(38) Eiseman, J. L.; Bai, L.; Jung, W. H.; Moura-Letts, G.; Day, B. W.; Curran, D. P. *J. Med. Chem.* **2008**, *51*, 6650–6653.
(39) Paterson, I.; Gardner, N. M.; Poullennec, K. G.; Wright, A. E. *Bioorg. Med. Chem. Lett.* **2007**, *17*, 2443–2447.
(40) Shin, Y.; Fournier, J. H.; Balachandran, R.; Madiraju, C.; Raccor, B. S.; Zhu, G.; Edler, M. C.; Hamel, E.; Day, B. W.; Curran, D. P. *Org. Lett.* **2005**, *7*, 2873–2876.
(41) (a) Michel, J.; Tirado-Rives, J.; Jorgensen, W. L. *J. Am. Chem. Soc.* **2009**, *131*, 15403–15411. (b) Barillari, C.; Taylor, J.; Viner, R.; Essex, J. W. *J. Am. Chem. Soc.* **2007**, *129*, 2577–2587. (c) Sleigh, S. H.; Seavers, P. R.; Wilkinson, A. J.; Ladbury, J. E.; Tame, J. R. H. *J. Mol. Biol.* **1999**, *291*, 393–415.
(42) (a) Alonso, H.; Gillies, M. B.; Cummins, P. L.; Bliznyuk, A. A.; Gready, J. E. *J. Comput.-Aided Mol. Des.* **2005**, *19*, 165–87. (b) Sato, H.; Shewchuk, L. M.; Tang, J. *J. Chem. Inf. Model.* **2006**, *46*, 2552–2562.
(43) Shanker, N.; Kingston, D. G. I.; Ganesh, T.; Yang, C.; Alcaraz, A. A.; Geballe, M. T.; Banerjee, A.; McGee, D.; Snyder, J. P.; Bane, S. *Biochemistry* **2007**, *46*, 11514–11527.
(44) Prussia, A. J.; Yang, Y.; Geballe, M. T.; Snyder, J. P. *ChemBioChem* **2010**, *11*, 101–109.